Insights into tribology from *in situ* nanoscale experiments

Tevis D.B. Jacobs[1], Christian Greiner[2], Kathryn J. Wahl[3], and Robert W. Carpick[4]

[1] Department of Mechanical Engineering and Materials Science, University of Pittsburgh, USA

[2] Christian Greiner, Karlsruhe Institute of Technology, and Institute for Applied Materials, Germany

[3] Kathryn J. Wahl, Chemistry Division, Naval Research Laboratory, USA

[4] Robert W. Carpick, Department of Mechanical Engineering and Applied Mechanics, University of Pennsylvania, USA

The published version of this article can be found at: doi:10.1557/mrs.2019.122
Full citation information is as follows:
Jacobs, T. D., Greiner, C., Wahl, K. J., & Carpick, R. W. (2019). Insights into tribology from in situ nanoscale experiments. MRS Bulletin, 44(6), 478-486.

Keywords:
tribology; nanoscale; surface chemistry; atomic force microscopy; transmission electron microscopy

Abstract:
Tribology—the study of contacting, sliding surfaces—seeks to explain the fundamental mechanisms underlying friction, adhesion, lubrication, and wear, and to apply this knowledge to technologies ranging from transportation and manufacturing to biomedicine and energy. Investigating the contact and sliding of materials is complicated by the fact that the interface is buried from view, inaccessible to conventional experimental tools. *In situ* investigations are thus critical in visualizing and identifying the underlying physical processes. This article presents key recent advances in the understanding of tribological phenomena made possible by *in situ* experiments at the nanoscale. Specifically, progress in three key areas is highlighted: (1) direct observation of physical processes in the sliding contact; (2) quantitative analysis of the synergistic action of sliding and chemical reactions (known as tribochemistry) that drives material removal; and (3) understanding the surface and subsurface deformations occurring during sliding of metals. The article also outlines emerging areas where *in situ* nanoscale investigations can answer critical tribological questions in the future.

Introduction

Tribology underlies the performance, safety, and reliability of nearly every mechanical system on land, at sea, and in space. The understanding and harnessing of tribological phenomena holds promise to address the 11% of annual energy consumption in transportation, utilities, and industrial applications lost due to friction and wear.[1] This is in addition to the opportunities to save billions of dollars annually lost to downtime of industrial equipment,[2] to eliminate billions of tons of CO_2 emissions annually,[3] and to significantly reduce human suffering caused by the failure of medical devices such as implants.[4]

Tribology depends on the physical, chemical, electrical, and system properties of the sliding materials, such as mechanical stiffness and strength, thermal and electrical conductance, hydrodynamic behavior, surface topography, material compatibility, temperature, sliding speed, and gas/fluid environment; in biological settings, a host of additional properties come in to play. Thus, the key parameters of interest such as the friction coefficient and wear rate are not material parameters, but rather, are system properties that vary with operational conditions. For newly engineered systems, or after a materials modification to an existing system, friction and wear performance are not currently predictable. Furthermore, the lack of direct observation of the sliding surfaces is a central obstacle to predicting performance and preventing failures. *In situ* techniques in tribology reveal the buried interfaces, as discussed in the 2008 issue of *MRS Bulletin* on the topic.[5] The ensuing decade has brought significant advances both at the larger scales (*e.g.,* Refs. 6–17) and at the nanoscale (*e.g.,* Refs.18–22); the latter is the focus of the present article.

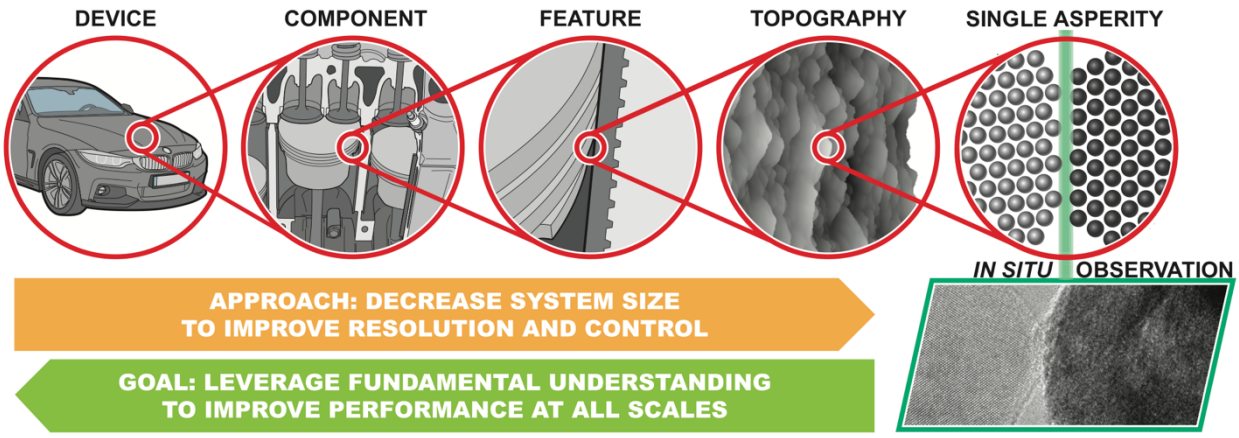

Figure 1. While tribological phenomena are complex and multiscale, fundamental understanding can be gained by reducing the system size to improve the control and measurement of local conditions. *In situ* nanotribology reveals the fundamental physical mechanisms and enables their systematic interrogation with the goal of informing design and optimization of larger-scale systems.

In situ nanotribology decreases the size scale of experiments to improve resolution and control over sliding conditions, with the goal of identifying and describing the underlying physical mechanisms (**Figure 1**). The fundamental understanding that is achieved from *in situ* nanoscale investigations can be generalized and harnessed at all length scales to improve tribological performance. Further, *in situ*

experiments can be directly matched with atomistic simulations, enabling atomic-scale understanding of results. By establishing and quantifying the physical relationships that relate structure, processing, and properties, the goal is to enable the rational design of components, devices, and systems to improve tribological performance.

Instrumentation for *in situ* nanotribology

In situ nanotribology experiments include the use of microscopy or an analysis technique to characterize interfacial processes during sliding. One primary approach is to use specialty specimen holders to directly observe the tribological testing of nanoscale bodies with an electron microscope.[23] This enables Ångström-scale resolution of morphology and surface topography. Simultaneously, the crystallographic structure, composition, and bonding chemistry can be characterized using analytical techniques such as nanobeam diffraction, energy dispersive x-ray spectroscopy (EDS), and electron energy loss spectroscopy (EELS). Another primary approach is to use atomic force microscopy (AFM) to perform both sliding and characterization. AFM enables precise control over the loading and sliding conditions, with simultaneous characterization of the surface's morphology and properties.[24] The environment can be varied widely, covering vacuum, ambient, controlled atmospheres, and liquid, including biologically compatible environments.

Another type of investigation (termed *quasi-in situ*) interrupts sliding to analyze surfaces. This includes sliding an AFM probe for some distance before removing it for high-resolution imaging of the tip or sample, or sliding a pin on a disk followed by the sectioning of surfaces for electron-microscopy analysis. Throughout this article, we discuss these *quasi-in situ* investigations as leading indicators, setting up the key scientific questions that will be answered by true *in situ* experiments.

Revealing the buried interface: Key results and future directions

Observations of novel phenomena

In situ tribology experiments were first demonstrated in the 1960s by the famous tribologist Bowden[25] who developed an *in situ* scanning electron microscope (SEM)-based indentation apparatus and studied small contacts of gold, copper, and aluminum; the *in situ* capability allowed Bowden and colleagues to observe that plastic deformation was negligible below a stress approaching the ideal strength of the metals tested; they then applied the instrumentation in a TEM.[26] Kato and co-workers[27] conducted *in situ* SEM-based wear studies of steel in 1988, directly observing a transition from plowing to wedge-forming to cutting as the degree of penetration increased. Shortly thereafter, Spence and co-workers developed a scanning tunneling microscope operating *in situ* inside a TEM, observing nanoscale compression of surfaces by the tip.[28,29]

More recently, both commercial and custom-built TEM-based instruments have revealed a wide range of phenomena for several different material classes. For instance, *in situ* TEM investigation of contact between noble metals demonstrated "cold welding" of asperities upon contact,[30,31] followed by liquid-like behavior during separation (discussed in more detail later). In the case of two-dimensional (layered) materials (*e.g.,* graphite, MoS_2), which are important solid lubricants, *in situ* TEM nanotribology has revealed rolling,[32] exfoliation,[33,34] and material transfer[35] during sliding. Another

transformative aspect of *in situ* electron microscopy is the ability to reveal chemistry and bonding of the materials at the interface. For example, EELS analysis revealed changes in the hybridization state of carbon-based materials during *in situ* contact. Merkle and co-workers[36] demonstrated a sliding-induced increase in the sp^2-to-sp^3 ratio of diamond-like carbon; conversely, Janei and co-workers[37] demonstrated a decrease in sp^2 content of soot particles after *in situ* compression.

Other recent work has leveraged the ability to work in biocompatible fluids, where *in situ* work has demonstrated links between tribological behavior and biological response.[38] This includes the effects of shear forces on the growth and proliferation of cells, as elucidated by approaches such as the direct observation of contact between a soft hydrogel cap and a layer of corneal epithelial cells imaged via fluorescence microscopy,[17] or the measurement of friction and shear force-induced inflammation of cells *in vitro*.[39]

These examples and many others demonstrate the power of *in situ* approaches to tribology. We next discuss selected studies in more detail that have advanced knowledge of tribology through direct observations at the nanoscale, and have uncovered or confirmed specific physical mechanisms underlying processes related to contact, adhesion, friction, and wear at all length scales.

The role of tribochemistry in material removal

Tribochemistry is the acceleration of chemical reactions at surfaces by sliding. Tribochemistry builds on the well-established field of mechanochemistry, which describes how mechanical forces can alter the kinetics of chemical reactions. However, the sliding action adds further complexity in the form of spatially and temporally varying loads, evolving surface morphology and chemistry, and the transport of reactants and products into and out of the contact region. In many applications, material removal by tribochemistry plays a primary role in sliding wear. A common theme that has emerged is the importance of thermally and tribologically activated chemical processes affecting wear. *In situ* investigations provide a way to understand, and even potentially predict and control, these wear processes.

Tribochemical wear in silicon and carbon-based materials

Significant wear and surface modification can occur in covalently bonded materials, even well below the fracture stress.[40] *Quasi-in situ* investigations using atomic force microscopy have demonstrated that material removal could be modeled using reaction rate theory.[41–45] Gotsmann and co-workers used high-speed AFM to study the wear of silicon[43] and carbon[44] nanoprobes with periodic adhesion measurements (as an indirect measure of probe radius) and *ex situ* electron microscopy (as a direct measure). They demonstrated that the wear was gradual, and could be described by combining reaction rate theory with an empirical model for friction stress, and the conical geometry of the probe.[43]

In situ nanoscale investigations have further advanced the understanding of tribochemical material removal. TEM observations of silicon AFM probes sliding on diamond (**Figure 2**a) demonstrated Ångström-scale recession of the silicon nanoprobe while the subsurface crystallography was

maintained.[18] Significant material removal occurred in the absence of fracture, plasticity (i.e., subsurface defects or permanent shape change), or observable debris (Figure 2b). The improved spatial and temporal resolution of the *in situ* TEM testing enabled the characterization of instantaneous tip shape and the quantification of the rate of atom removal. By combining the asperity shape with subnanonewton force resolution, the local and instantaneous mean contact stress could be computed. Together, these measurements provided direct evidence that sliding wear occurred through surface reactions with an Arrhenius dependence on local stress, (Figure 2c) where the atomic reaction rate Γ (with units of s^{-1}) is given by:[45]

$$\Gamma = \Gamma_0 exp\left(-\frac{\Delta G_{act}}{k_B T}\right), \quad (1)$$

where the prefactor Γ_0 includes the effective attempt frequency of the reaction, which is related to atomic vibration frequencies, ΔG_{act} is the Gibbs free energy of activation for the rate-limiting reaction in the process, k_B is Boltzmann's constant, and T is the absolute temperature. The fit to the data assumes that ΔG_{act} is influenced by stress according to:

$$\Delta G_{act} = \Delta U_{act} - \sigma \Delta V, \quad (2)$$

where ΔU_{act} is the internal activation energy (energy barrier in the absence of stress), σ is the mean value of the stress component affecting the activation barrier, and ΔV is the activation volume. In this case, σ was taken as the compressive stress (which assists in covalent bond formation across the interface); however, because the interfacial shear stress depends on the compressive pressure, it is difficult to distinguish which stress is "activating" in a given situation.

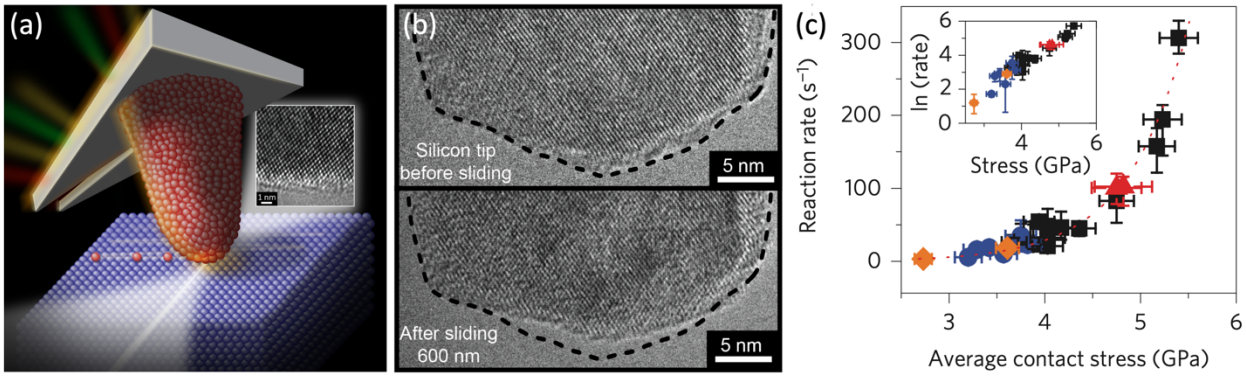

Figure 2. The sliding of a silicon atomic force microscope probe on diamond in a transmission electron microscope (a) enables characterization of the evolving shape and structure during wear (b).[46] Combining the wear data with real-time load measurements (c) enables the direct demonstration of reaction rate theory (Equation 1) and the extraction of activation parameters for low-load wear of silicon.[18] The inset in (c) shows that the data collapses to a straight line on a log-linear plot.

AFM wear experiments with *in situ* tip-based heating were performed on functionalized graphene surfaces (**Figure 3**) to further interrogate the stress-dependent kinetics of bond breaking and the effect of temperature on bond-scission dynamics.[19,47] Real-time friction measurements were used as an *in*

situ measurement of molecular-scale material removal, and the heated AFM probes directly applied temperature ramps to examine temperature-dependent rates of material loss.[47] In contrast to prior experiments that assumed thermal activation, first-order reaction kinetics were used to verify an Arrhenius dependence of the material removal rate on inverse temperature. Additionally, by controlling applied load and contact time, the authors were able to measure the different kinetics of oxygen-, fluorine-, and hydrogen-functionalized graphene.[19]

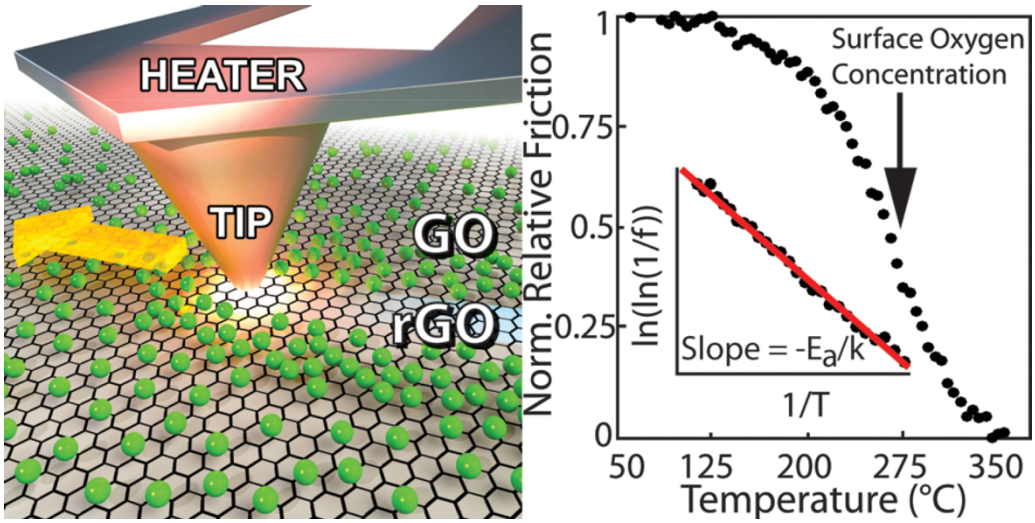

Figure 3. Temperature-controlled sliding experiments used the friction force f as a real-time measurement of surface coverage of functional groups on graphene. Here, the removal of oxygen groups from graphene oxide (GO) produces reduced graphene oxide (rGO). By varying the temperature, the thermal activation was directly confirmed and the activation parameters of bond scission were extracted. In this graphic, E_a is activation energy and k is Boltzmann's constant. Reprinted with permission from Reference 47. © 2017 American Chemical Society.

The importance of these stress-controlled bonding reactions were also demonstrated for adhesive contacts even in the absence of sliding. *In situ* TEM experiments of amorphous carbon tips in contact with diamond showed gradual material removal, and fluctuations in the adhesion force due to covalent bond formation during contact.[48] Finally, interrupted (*quasi-in situ*) imaging of amorphous carbon tips in sliding contact with diamond revealed a load-dependent transition from an exponential dependence on stress (the Arrhenius-like behavior described in Eqs. 1-2) to the linear dependence described by the Archard equation for wear.[49]

Taken together, these recent *in situ* nanoscale investigations established stress-modified thermally activated bond-breaking as the key framework for describing low-load wear behavior of covalent materials. The predictive power of this framework, and its limits of applicability, are still being actively explored.

Tribochemical buildup and removal of antiwear additives

Industrial lubricants contain a substantial fraction (up to ca. 10 wt%) of additives for important functions, including reducing boundary friction, controlling viscosity, and reducing wear. Particularly important is the family of zinc dialkyldithiolphosphate (ZDDP) additives, which are used in every commercial lubricant for internal combustion engines. These tribochemically active molecules reduce wear and corrosion by forming thin protective films ("tribofilms") through adsorption and confinement at contacting asperities, followed by force-induced dissociation and subsequent reactions (**Figure 4**).[20,50,51] ZDDPs are inexpensive and highly effective, but contain sulfur and phosphorous that poison catalytic converters, thereby increasing harmful emissions. The automotive industry has for decades sought a suitable replacement but has not yet succeeded. One reason is that the underlying tribochemical behavior at the asperity level was not well understood. Macroscopic, *ex situ,* and *quasi-in situ* studies[51–55] have elucidated the structure and composition of these films; experiments have shown that compressive[56] and shear[50] forces are crucial for film formation, but insights to explain the tribofilms' graded structure and self-limiting growth (at approximately 100-nm thickness) are long-standing challenges.

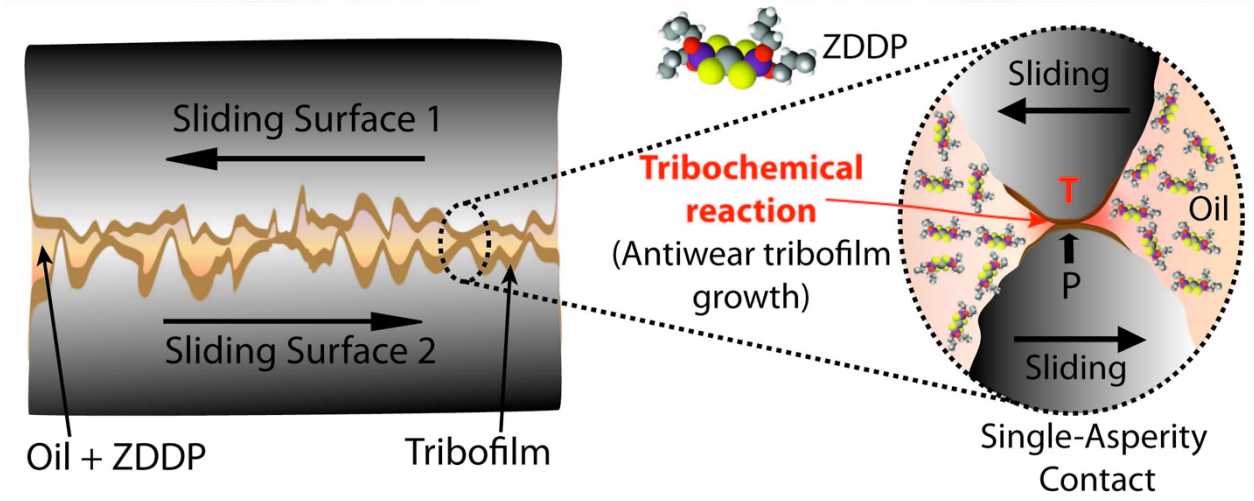

Figure 4. A challenge in understanding force-dependent reactions is that the contacting surfaces are not atomically smooth, with energy dissipated largely at nanoscale asperity-asperity contacts. This affects the reactions of molecules such as zinc dialkyldithiolphosphate that undergo shear-assisted reactions at the single-asperity scale forming surface-bound films.[20] Image courtesy of N.N. Gosvami, Indian Institute of Technology, Delhi.

Gosvami et al. recently developed an AFM method where tribofilms are created *in situ* while simultaneously probing nanoscale properties including morphology, friction, and wear (**Figure 5**a).[57] A single-asperity contact is formed between an AFM tip and a flat sample submerged in a conventional AFM liquid cell containing the lubricant. Alternatively, multi-asperity contacts can be formed by using a rough microscale colloidal tip.[57] Applied force, sliding velocity, and temperature can be varied, and thus nucleation and growth of tribofilms are mapped in real-time against shear rate, stress, and temperature. Gosvami et al.[20] heated the ZDDP-containing polyalphaolefin oil to 80–140°C during

sliding experiments, which were performed for a range of normal loads. Sliding-induced ZDDP tribofilms grew at a rate that was well-described by Equation 1 (Figure 5b). Again, σ was assumed to be the initial compressive contact pressure, but shear stress could in fact be controlling the reaction, as shown in macroscopic studies by Zhang and Spikes;[50] the model holds if the shear stress is proportional to the normal stress. Fitting of Equations (1) and (2) (Figure 5b–c) gave values of ΔU_{act} = 0.8 ± 0.2 eV and ΔV = 3.8 ± 1.2 Å^3, consistent with a molecular-scale process.

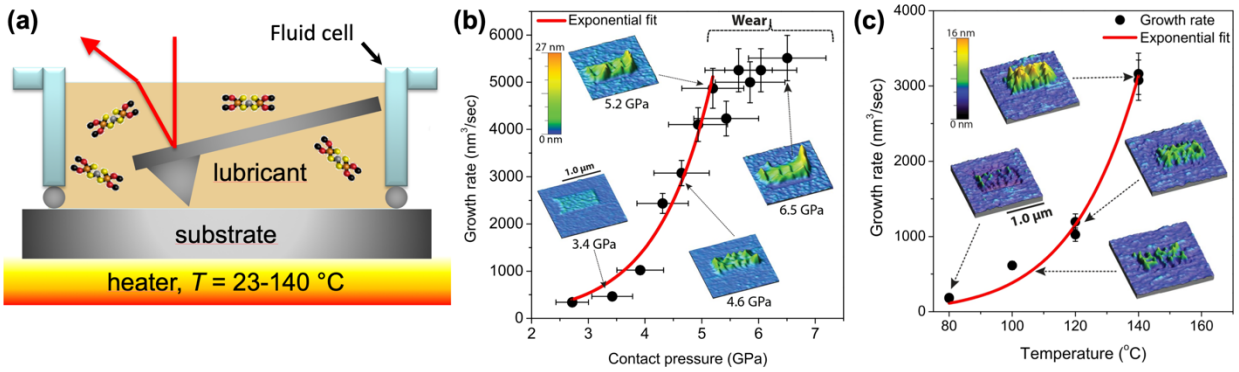

Figure 5. (a) Schematic of the atomic force microscopy setup immersed in a lubricant (zinc dialkyldithiolphosphate [ZDDP] additive molecules schematically shown) used for *in situ* tribofilm formation. (b) ZDDP tribofilm growth rate versus mean applied normal contact stress at constant temperature, fit with an exponential (stress-activated) function (Equations 1 and 2). (c) Tribofilm growth rate versus temperature at constant normal stress, also fit with an exponential function, Insets to (b) and (c): log of growth rate versus stress and temperature, respectively. (b, c) Reprinted with permission from Reference 20. © 2015 AAAS.

Stress-activated growth explains why ZDDP-derived tribofilms have a graded structure and a self-limiting thickness. Reduced contact pressure—resulting from the tribofilm's low modulus—limits the degree of cross-linking and other tribofilm-forming reactions, resulting in a graded structure with progressively less cross-linking and a lower modulus, thus further reducing the contact pressure. The growth rate thus reduces and eventually tapers off as the film grows, a sort of "cushioning" effect, which is supported by a recent asperity-based kinetic model.[58] Dorgham et al.[59] further demonstrated the versatility of this method, when they compared ZDDP with an ashless (metal-free) DDP, finding that the reaction order is different, indicating that the tribochemical reaction pathways depend significantly on the molecule's structure. This *in situ* method has also been used to form and study tribofilms derived from solid ZrO_2 nanoparticle additives in oils,[60] and applied to form patterned tribofilms on surfaces, termed "nanotribological printing."[61]

Tribocorrosion

The synergism between chemistry and material removal is even more severe in corrosive environments, including biomedical implants,[62] nuclear power plants,[63] and marine environments.[64] Even in corrosion-resistant alloys, sliding action causes repetitive loss of protective surface films, resulting in the loss of metal ions to repassivate the worn surface and thereby accelerating material

degradation.[65] Corrosion-resistant metals typically contain costly alloying elements such as Ni and Co, and can have complex microstructures with carbide or nitride inclusions. Besides solution chemistry and sliding contact conditions, the wear-corrosion synergy is controlled by factors such as composition, applied potential, applied or residual stresses, and fatigue resistance.[9,66–68] The mechanisms by which local material properties influence tribocorrosion processes are underexplored.

The state-of-the-art involves breakthroughs from *quasi-in situ* investigations. Malayoglu and Neville[69] used examination of worn surfaces by AFM to show that the preferential removal of Co-rich matrix material was more pronounced on cast versus hot isostatically pressed (HIPed) CoCr alloys. Wang et al.[70] revealed that preferential dissolution at the boundary region between carbides and the CoCrMo matrix accelerates abrasive wear in medical implant alloys. Shockley et al.[16] demonstrated, for an aged duplex stainless steel, that sliding wear initiated runaway pitting corrosion in susceptible phases, which did not occur in the absence of sliding.

These advances motivate locally probing fundamental material processes of sliding wear in corrosive environments. For instance, while repassivation kinetics is modeled in its simplest form using Faraday's Law[65] and has been explored for microscale scratching by diamond tips,[63] the periodic removal and repassivation of oxide films that occurs in tribological sliding is not well understood. Further, current tribocorrosion modeling relies on the assumption of full oxide removal,[65] while real-world multi-asperity contacts may experience only partial removal of the oxide. Fully *in situ* nanoscale investigations based on electrochemical scanning probe microscopy represent a promising pathway for enriching our understanding of the local processes in tribocorrosion.

Surface and subsurface processes in metals

The majority of tribologically loaded engineering components are metals, including noble metals for specialty applications and oxide-forming metals for general use. The understanding of deformation and energy dissipation in these metals is being significantly advanced by *in situ* and *quasi-in situ* investigations.

Surface adhesion (or cold-welding) of metal contacts

Adhesive wear, often referred to as galling, typically results from the combined action of friction and adhesion on sliding pairs, and can be a source of significant energy dissipation and material removal or degradation. The spontaneous bonding of metals has been extensively studied using the approach of mechanically controllable break junctions, where wires are pulled to breaking in a high-vacuum environment and then brought back into contact. Many of these contact-and-separation experiments have been *quasi-in situ,* where electrical current was recorded as an indirect measure of junction size; these have demonstrated the liquid-like separation and reforming of the contact (sometimes referred to as cold welding).[71–73] As mentioned earlier, fully *in situ* nanoscale experiments of nanoscale junctions[30,31] established that many noble-metal contacts separate in a progressively thinning ligament that culminates, in some cases, in a single-atom chain before separation. These results have been

confirmed for tribologically relevant contacts, including gold and silver.[21,74–77] This liquid-like behavior has even been observed in nonmetallic contacts of aluminum oxide[78] and silicon carbide.[79] The fundamental understanding of this liquid-like contact behavior has been advanced using *in situ* nanoscale investigations. Using contact and sliding tests in the TEM on silver,[80] gold,[81] and oxide-free tin[22] nanocontacts, it was shown that this deformation was accommodated through the motion of surface steps in the material surrounding the contact. After separation, asperities regained a similar resting shape regardless of the amount of deformation induced. This indicated deformation that was mediated by surface diffusion (**Figure 6**a–b), analogous to Coble creep, where time-dependent deformation in load-bearing bulk materials occurs via atomic diffusion along grain boundaries.

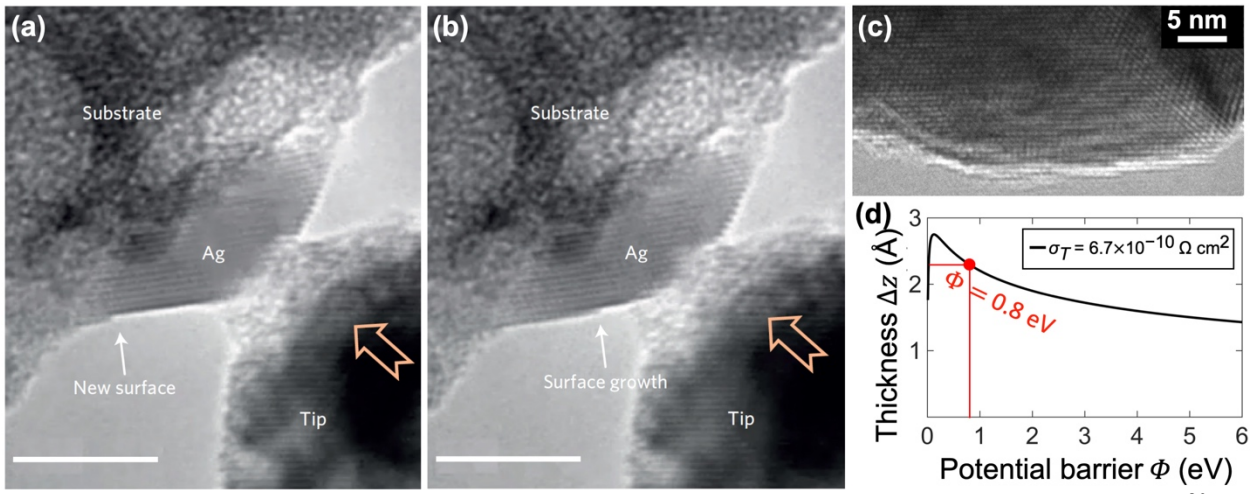

Figure 6. *In situ* transmission electron microscopy compression of silver contacts shows[80] that deformation is accommodated through the motion of surface steps (a, b). (The scale bars are 5 nm in length.) However, subsurface defect-based plasticity is observed[85] in platinum nanocontacts (c), and real-time electrical measurements[86] are consistent with the presence of atomic-scale surface layers (d), which may disrupt surface diffusion. (a, b) were reproduced with permission from Reference 80, © 2014 Nature Publishing Group. (c, d) were reproduced with permission from Reference 86, © 2018 IOP Publishing.

Tin contacts were described using a Coble-creep model that relates the stress σ to the strain-rate $\dot{\varepsilon}$:[22]

$$\dot{\mathrm{E}} = K\frac{\delta_S D_S \Omega}{D^3 k_B T}\sigma, \tag{3}$$

where D is the characteristic dimension (e.g., diameter of the asperity) and K is a dimensionless constant. The material properties are described by surface diffusivity D_S, nominal surface layer thickness δ_S, and atomic volume Ω. Li and co-workers combined *in situ* nanotribology experiments with simulations to delineate regimes where deformation will be liquid-like (what the authors call diffusive plasticity[82]) or dislocation-mediated (termed displacive plasticity[82]). Both processes can occur simultaneously,[83] but a criterion based on MD simulations and *in situ* nanoscale experiments determines which process will dominate.[84] In dislocation-based plasticity, "smaller is stronger," as

expressed by the Hall–Petch relationship, $\sigma_{flow} = \sigma_0 + kD^{-1/2}$, where σ_0 and k are constants. In contrast, in surface diffusion-dominated deformation with a specific material, temperature, and flow rate, the flow stress is governed by $\sigma_{flow} = \sigma_0 + kD^3$, which indicates that "smaller is much weaker."

Separate *in situ* TEM adhesion experiments demonstrated the critical role that surface chemistry plays in the deformation of platinum nanocontacts. Liquid-like diffusive behavior is not observed in self-mated platinum nanocontacts,[85] likely due to the presence of surface monolayers of oxygen or carbonaceous material (Figure 6c–d),[86] which is consistent with atomistic simulations.[87] These surface layers prevent the motion of the surface steps that are required for diffusive plasticity. Surprisingly, these surface layers are not removed by mechanical means, even with loading and sliding in vacuum.[86]

Subsurface dislocation processes in metal contacts

Dislocation-mediated processes in the subsurface region of a contact are critical for understanding deformation and energy dissipation in metals in sliding contact.[88] The movement and self-organization of dislocations leads to a dynamic and complex subsurface microstructure.[89,90] The structure–properties relationship of a tribological contact was recently described as a feedback loop between grain size, friction, and surface stresses.[91] This suggests opportunities to tailor alloys for tribological applications; however, doing so requires revealing the mechanisms governing these microstructural processes. *In situ* TEM experiments of moving tribological contacts represent an important opportunity, yet such experiments are very challenging, both in instrumentation and in application to real-world conditions. For instance, *in situ* TEM requires electron transparency and thus ultrathin widths, yet these small dimensions introduce image forces from the free surfaces and other thin-film effects that strongly affect results.[92]

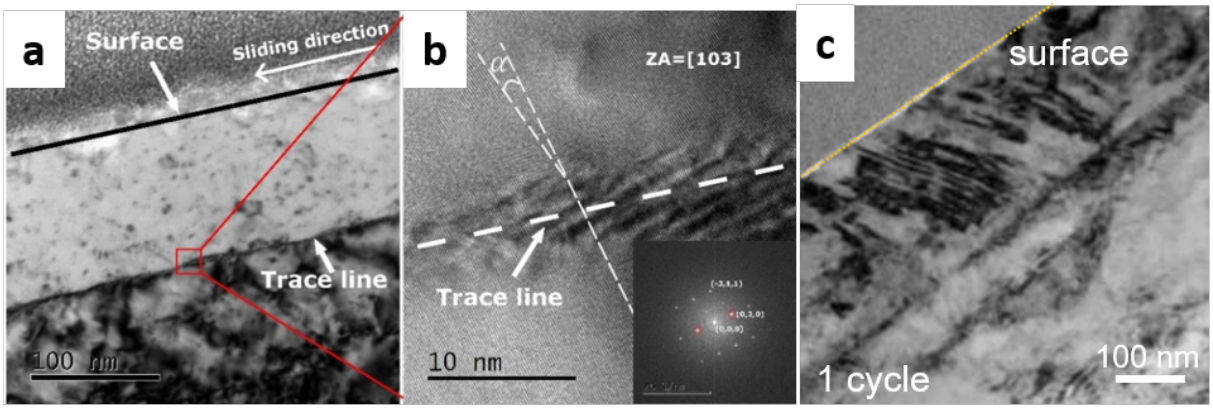

Figure 7. Dislocation self-organization during the very early stages of sliding leads to a horizontal small-angle grain-boundary-like feature, which can be observed using transmission electron microscopy after only a single sliding event (a, b). The foil was tilted to a [103] zone axis (ZA) .[93] The line-like feature was found to be a boundary separating regions that accommodate shear differently, with dislocation motion dominant below the line and twinning dominant above, as shown in (c).[95]

Critical advances have been established using *quasi-in situ* tribological experiments, with high-resolution TEM analysis of the subsurface structure. Experiments on annealed copper revealed that after only one mild pass of a counter body, dislocations self-organized and formed a horizontal dislocation feature similar to a small-angle grain boundary 150 nm under the surface (**Figure 7**a–b).[93] This feature was the precursor to microstructural discontinuities observed upon further sliding[15,94] and also separated the regions where deformation occurred primarily through twinning or through dislocation motion (Figure 7c).[93,95] With increasing sliding distance, large quantities of dislocations are emitted from and through the sliding contact to a depth of several micrometers. Dislocations self-organized, first into networks of geometrically necessary dislocations, then into sub-grains, and ultimately into a fine-grained "tribo-layer."[96–98] This method of interrupted sliding on non-noble metals has also helped to understand how pearlitic steels accommodate a tribological strain through a sequence of different processes[99] and has shed light on tribologically induced oxidation.[100]

At the same time, this current state of the art is not satisfactory. Postmortem analyses inherently allow different interpretations for how the observed structures have been achieved. For instance, MD simulations[101] have suggested the importance of the Bauschinger effect, where the back-stresses of dislocations that are induced during loading in the forward direction serve to aid the activation of dislocation slip in the reverse direction. Complete understanding of real-time processes requires *in situ* nanoscale analysis. A recent first step in this direction linked *in situ* TEM with MD to demonstrate that the contact area in a metal nanocontact can be up to 160% larger than predicted by classical continuum theories due to dislocation nucleation and motion, even for contacts without irreversible shape change.[85] These results demonstrate the need to closely consider dislocation activity even in pseudoelastic contacts, and more broadly, show the potential for future *in situ* TEM testing of subsurface deformation of metal nanocontacts.

Summary and outlook

In situ nanotribology has enabled breakthroughs in the understanding of fundamental mechanisms in tribology, and it represents a powerful platform for current and future advances in the field. This progress has been facilitated by advancements in electron microscopy, where aberration-correction equipment has enabled single-atom resolution and also larger physical pole-piece gaps to accommodate an increasing range of *in situ* tools. *In situ* tribology investigations have only just begun to leverage the analytical capabilities of electron microscopy to analyze the chemistry and bonding at the interface. The proliferation of environmental TEM equipment is ideally suited for tribological experiments—by enabling the introduction of humid or gas environments during testing, experiments can more accurately reflect real-world conditions in many tribological contacts. However, to take full advantage of these TEM advances, further improvements are required for the *in situ* TEM test platforms. Key limitations of existing test platforms include: vibration and drift, which limit image quality and precision of movement; limited tilt range, which prevents 3D characterization using tomographic techniques; and the use of complex or custom fixturing, which significantly limits throughput and thus sample size and statistical significance of results. There are promising approaches to address some of these limitations, including integrating the test surfaces directly into a

microelectromechanical systems-based chip to improve stability;[102] however, further progress is needed, especially using commercial *in situ* TEM testers, to fully leverage the advantages of modern TEM.

There is still much work to be done to apply the mechanisms revealed using *in situ* nanoscale testing to bulk conditions. For example, friction coefficients and wear rates for the same material can differ by more than an order of magnitude when measured at nanoscopic and macroscopic dimensions.[103] These inconsistencies reflect important differences in conditions, such as: wearless sliding in an AFM as compared to wear-inducing sliding in bearings; or dry *in situ* TEM tests as compared to lubricated engine conditions; or an adhesive single asperity under gigapascals of contact stress as compared to a (nominally) flat contact under apparent stresses that are orders of magnitude lower, and where contact occurs at many asperities simultaneously. In many cases, the underlying physical processes are related across all scales of tribology, but differences in conditions can modify the mechanisms and their kinetics and energetics.

Three key needs stand out for further scientific advancements of tribology in the future. First, true *in situ* investigations are needed in cases where the current state-of-the-art is *quasi-in situ* investigation. For example, the *quasi-in situ* investigation of plasticity in a sliding contact must be advanced through the real-time observation of dislocation creation and self-organization. Second, while significant progress has been made in single-asperity experiments and atomistic modeling of nanoscale contacts, the field is still lacking the multi-scale modeling and combined multi-resolution experiments needed to bridge length and time scales and to directly apply fundamental insights to macroscale components. This includes work on biological systems, where many opportunities abound.[38] Third, significant improvements are needed in the description and understanding of surface topography and its effect on properties. Scaling-up of knowledge requires not just an increase in the size of the contacting components, but also a more complete understanding of the statistical distribution and behavior of roughness at all scales. Continued advancement in these three areas will enable the ultimate goal of rational, science-based improvement of the tribological performance of sliding components in real-world devices.

Acknowledgments

T.D.B.J. acknowledges support from the National Science Foundation through Award CMMI-1536800. C.G. acknowledges funding by the German Research Foundation under Project GR 4174/1 and by the European Research Council (ERC) under Grant No. 771237, TriboKey. K.J.W. acknowledges support from the Base Program at the Naval Research Laboratory via the Office of Naval Research. R.W.C. acknowledges support from the National Science Foundation through Awards CMMI-1728360 and CMMI-1761874, and from AFOSR/AOARD though Award FA2386–18–1-4083. The authors wish to thank W.G. Sawyer, N.N. Gosvami, R. Bernal, F. Dassenoy, and J. Felts for useful discussion.

References

1. R.W. Carpick, A. Jackson, W.G. Sawyer, N. Argibay, P. Lee, A. Pachon, R.M. Gresham, *Tribol. Lubr. Technol.* **72**, 44 (2016).
2. H.P. Jost, *Wear* **136**, 1 (1990).
3. K. Holmberg, A. Erdemir, *Friction* **5**, 263 (2017).
4. S. Affatato, M. Spinelli, M. Zavalloni, C. Mazzega-Fabbro, M. Viceconti, *Med. Eng. Phys.* **30**, 1305 (2008).
5. W.G. Sawyer, K.J. Wahl, *Mater. Res. Soc. Bull.* **33**, 1145 (2008).
6. A. Ovcharenko, G. Halperin, I. Etsion, *Wear* **264**, 1043 (2008).
7. A. Ovcharenko, G. Halperin, I. Etsion, *J. Tribol.* **131**, 011404 (2009).
8. J.M. Urueña, S.M. Hart, D.L. Hood, E.O. McGhee, S.R. Niemi, K.D. Schulze, P.P. Levings, W.G. Sawyer, A.A. Pitenis, *Tribol. Lett.* **66**, 141 (2018).
9. A.H. Zavieh, N. Espallargas, *Tribol. Int.* **99**, 96 (2016).
10. A. Ovcharenko, I. Etsion, *J. Tribol.* **131**, 031602 (2009).
11. B.A. Krick, J.R. Vail, B.N.J. Persson, W.G. Sawyer, *Tribol. Lett.* **45**, 185 (2012).
12. K.G. Rowe, A.I. Bennett, B.A. Krick, *Tribol. Int.* **62**, 208 (2013).
13. A.I. Bennett, K.L. Harris, K.D. Schulze, J.M. Urueña, A.J. McGhee, A.A. Pitenis, M.H. Müser, T.E. Angelini, W.G. Sawyer, *Tribol. Lett.* **65**, 134 (2017).
14. B. Weber, T. Suhina, T. Junge, L. Pastewka, A.M. Brouwer, D. Bonn, *Nat. Commun.* **9**, 888 (2018).
15. S. Korres, T. Feser, M. Dienwiebel, *Acta Mater.* **60**, 420 (2012).
16. J.M. Shockley, D.J. Horton, K.J. Wahl, *Wear* **380–381**, 251 (2017).
17. S.L. Marshall, K.D. Schulze, S.M. Hart, J.M. Urueña, E.O. McGhee, A.I. Bennett, A.A. Pitenis, C.S. O'Bryan, T.E. Angelini, W.G. Sawyer, *Biotribology* **11**, 69 (2017).
18. T.D.B. Jacobs, R.W. Carpick, *Nat. Nanotechnol.* **8**, 108–112 (2013).
19. J.R. Felts, A.J. Oyer, S.C. Hernandez, K.E. Whitener, J.T. Robinson, S.G. Walton, and P.E. Sheehan, *Nat. Commun.* **6**, 6467 (2015).
20. N.N. Gosvami, J.A. Bares, F. Mangolini, A.R. Konicek, D.G. Yablon, R.W. Carpick, *Science* **348**, 102 (2015).
21. J. Wang, F. Sansoz, J. Huang, Y. Liu, S. Sun, Z. Zhang, S.X. Mao, *Nat. Commun.* **4**, 1742 (2013).
22. L. Tian, J. Li, J. Sun, E. Ma, Z.W. Shan, *Sci. Rep.* **3**, 1 (2013).
23. T.D.B. Jacobs, A. Martini, *Appl. Mech. Rev.* **69**, 060802 (2017).
24. I. Szlufarska, M. Chandross, R.W. Carpick, *J. Phys. D Appl. Phys.* **41**, 123001 (2008).
25. N. Gane, F.P. Bowden, *J. Appl. Phys.* **39**, 1432 (1968).
26. N. Gane, *Proc. R. Soc. London. A* **317**, 367 (1970).
27. K. Hokkirigawa, K. Kato, Z.Z. Li, *Wear* **123**, 241 (1988).
28. W.K. Lo, J.C.H. Spence, *Ultramicroscopy* **48**, 433 (1993).
29. J.C.H. Spence, W. Lo, M. Kuwabara, *Ultramicroscopy* **33**, 69 (1990).
30. Y. Kondo, K. Takayanagi, *Phys. Rev. Lett.* **79**, 3455 (1997).
31. H. Ohnishi, Y. Kondo, K. Takayanagi, *Nature* **395**, 780 (1998).
32. I. Lahouij, F. Dassenoy, L. Knoop, J.-M. Martin, B. Vacher, *Tribol. Lett.* **42**, 133 (2011).
33. I. Lahouij, F. Dassenoy, B. Vacher, J.-M. Martin, *Tribol. Lett.* **45**, 131 (2011).
34. J.P. Oviedo, K.C. Santosh, N. Lu, J.G. Wang, K. Cho, R.M. Wallace, M.J. Kim, *ACS Nano* **9**, 1543 (2015).
35. A.P. Merkle, L.D. Marks, *Appl. Phys. Lett.* **90**, 1 (2007).
36. A.P. Merkle, A. Erdemir, O.L. Eryilmaz, J.A. Johnson, L.D. Marks, *Carbon,* **48**, 587 (2010).
37. I.Z. Jenei, F. Dassenoy, T. Epicier, A. Khajeh, A. Martini, D. Uy, H. Ghaednia, A. Gangopadhyay, *Nanotechnology* **29**, 85703 (2018).
38. A.A. Pitenis, J.M. Urueña, E.O. McGhee, S.M. Hart, E.R. Reale, J. Kim, K.D. Schulze, S.L. Marshall, A.I. Bennett, S.R. Niemi, T.E. Angelini, *Tribol. Mater. Surf. Interfaces* **11**, 180 (2017).
39. A.A. Pitenis, J.M. Urueña, T.T Hormel, T. Bhattacharjee, S.R. Niemi, S.L. Marshall, S.M. Hart, K.D. Schulze, T.E. Angelini, W.G. Sawyer, *Biotribology* **11**, 77 (2017).
40. L. Yang, Y.Y. Lua, M.V. Lee, M.R. Linford, *Acc. Chem. Res.* **38**, 933 (2005).
41. W. Maw, F. Stevens, S.C. Langford, J.T. Dickinson, *J. Appl. Phys.* **92**, 5103 (2002).
42. P.E. Sheehan, *Chem. Phys. Lett.* **410**, 151 (2005).
43. B. Gotsmann, M.A. Lantz, *Phys. Rev. Lett.* **101**, 125501 (2008).

44. H. Bhaskaran, B. Gotsmann, A. Sebastian, U. Drechsler, M.A. Lantz, M. Despont, P. Jaroenapibal, R.W. Carpick, Y. Chen, K. Sridharan, *Nat. Nanotechnol.* **5**, 181 (2010).
45. T.D.B. Jacobs, B. Gotsmann, M.A. Lantz, R.W. Carpick, *Tribol. Lett.* **39**, 257 (2010).
46. R.W. Carpick, T.D.B. Jacobs, *Microsc. Microanal.* **20**, 1542 (2014).
47. S. Raghuraman, M.B. Elinski, J.D. Batteas, J.R. Felts, *Nano Lett.* **17**, 2111 (2017).
48. R.A. Bernal, P. Chen, J.D. Schall, J.A. Harrison, Y.R. Jeng, R.W. Carpick, *Carbon* **128**, 267 (2018).
49. Y. Shao, T.D.B. Jacobs, Y.J. Jiang, K.T. Turner, R.W. Carpick, M.L. Falk, *ACS Appl. Mater. Interfaces* **9**, 35333 (2017).
50. J. Zhang, H. Spikes, *Tribol. Lett.* **63**, 24 (2016).
51. H. Spikes, *Tribol. Lett.* **17**, 469 (2004).
52. M. Aktary, M.T. McDermott, G.A. McAlpine, *Tribol. Lett.* **12**, 155 (2002).
53. J.M. Martin, T. Onodera, C. Minfray, F. Dassenoy, A. Miyamoto, *Faraday Discuss.* **156**, 311 (2012).
54. C. Grossiord, J.M. Martin, T. Le Mogne, T. Palermo, *Tribol. Lett.* **6**, 171 (1999).
55. G. Pereira, A. Lachenwitzer, D. Munoz-Paniagua, M. Kasrai, P.R. Norton, M. Abrecht, P.U.P.A. Gilbert, *Tribol. Lett.* **23**, 109 (2006).
56. N.J. Mosey, M.H. Müser, T.K. Woo, *Science* **307**, 1612 (2005).
57. N.N. Gosvami, J. Ma, R.W. Carpick, *Tribol. Lett.* **66**, 154 (2018).
58. A. Akchurin, R.A. Bosman, *Tribol. Lett.* **65**, 59 (2017).
59. A. Dorgham, P. Parsaeian, A. Azam, C. Wang, A. Morina, A. Neville, *Tribol. Int.* **133,** 288 (2019).
60. H.S. Khare, I. Lahouij, A. Jackson, G. Feng, Z.Y. Chen, G.D. Cooper, R.W. Carpick*, ACS Appl. Mater. Interfaces* **10**, 40335 (2018).
61. H.S. Khare, N.N. Gosvami, I. Lahouij, Z.B. Milne, J.B. McClimon, R.W. Carpick, *Nano Lett.* **18**, 6756 (2018).
62. J.L. Gilbert, *Corrosion* **73**, 1478 (2017).
63. W. Zhang, A.G. Carcea, R.C. Newman, *Faraday Discuss.* **180**, 233 (2015).
64. R.J.K. Wood, *Wear* **376**, 893 (2017).
65. D. Landolt, S. Mischler, *Tribocorrosion of Passive Metals and Coatings.* (*Elsevier*, 2011).
66. V. Swaminathan, J.L. Gilbert, *J. Biomed. Mater. Res. A* **101**, 2602 (2013).
67. C.B. Von der Ohe, R. Johnsen, N. Espallargas, *Wear* **271**, 2978 (2011).
68. A.H. Zavieh, N. Espallargas, *Tribol. Int.* **103**, 368 (2016).
69. U. Malayoglu, A. Neville, *Wear* **255**, 181 (2003).
70. Z. Wang, Y. Yan, L. Xing, Y. Su, L. Qiao, *Tribol. Int.* **113**, 370 (2017).
71. M. Tsutsui, K. Shoji, M. Taniguchi, T. Kawai, *Nano Lett.* **8**, 345 (2008).
72. N. Agrait, *Phys. Rep.* **377**, 81 (2003).
73. U. Landman, W.D. Luedtke, N. Burnham, R. Colton, *Science* **248**, 454 (1990).
74. A.J. Lockwood, K. Anantheshwara, M.S. Bobji, B.J. Inkson, *Nanotechnology* **22**, 105703 (2011).
75. A.P. Merkle, L.D. Marks, *Wear* **265**, 1864 (2008).
76. T. Sato, T. Ishida, L. Jalabert, H. Fujita, *Nanotechnology* **23**, 505701 (2012).
77. Y. Lu, J.Y. Huang, C. Wang, S. Sun, J. Lou, *Nat. Nanotechnol.* **5**, 218 (2010).
78. Y. Yang, A. Kushima, W. Han, H. Xin, J. Li, *Nano Lett.* **18**, 2492 (2018).
79. Z. Zhang, J. Cui, B. Wang, H. Jiang, G. Chen, J. Yu, C. Lin, C. Tang, A. Hartmaier, J. Zhang, J. Luo, *Nanoscale* **10**, 6261 (2018).
80. J. Sun, L. He, Y.C. Lo, T. Xu, H. Bi, L. Sun, Z. Zhang, S.X. Mao, J. Li, *Nat. Mater.* **13**, 1007 (2014).
81. T. Ishida, T. Sato, S. Nabeya, K. Kakushima, H. Fujita, *Jpn. J. Appl. Phys.* **50**, 077201 (2011).
82. S. Suresh, J. Li, *Nature* **456**, 716 (2008).
83. P. Liu, X. Wei, S. Song, L. Wang, A. Hirata, T. Fujita, X. Han, Z. Zhang, M. Chen, *Acta Mater.* **165**, 99 (2018).
84. W. Guo, Z. Wang, J. Li, *Nano Letters* **15**, 6582 (2015).
85. S.B. Vishnubhotla, R. Chen, S.R. Khanal, A. Martini, T.D.B. Jacobs, *Nanotechnology* **30**, 35704 (2019).
86. S.B. Vishnubhotla, R.M. Chen, S.R. Khanal, J. Li, E.A. Stach, A. Martini, T.D.B. Jacobs*, Nanotechnology* **30**, 45705 (2019).
87. F. Yang, R.W. Carpick, D.J. Srolovitz, *ACS Nano* **11**, 490 (2017).
88. F.P. Bowden, D. Tabor, *Friction and lubrication of solids* (Oxford University Press, 1950)
89. D.A. Rigney, M.G.S. Naylor, R. Divakar, L.K. Ives, *Mater. Sci. Eng.* **81**, 409 (1986).
90. D.A. Hughes, N. Hansen, *Phys. Rev. Lett.* **87,** 135503 (2001)

91. N. Argibay, M. Chandross, S. Cheng, J.R. Michael, *J. Mater. Sci.* **52,** 2780 (2017).
92. E. Arzt, *Acta Mater.* **46,** 5611 (1998).
93. C. Greiner, Z. Liu, R. Schneider, L. Pastewka, P. Gumbsch, *Scr. Mater.* **153,** 63 (2018).
94. A. Emge, S. Karthikeyan, H.J. Kim, D.A. Rigney, *Wear* **263**, 614 (2007).
95. X. Chen, R. Schneider, P. Gumbsch, C. Greiner, *Acta Mater.* **161,** 138 (2018).
96. C. Greiner, Z. Liu, L. Strassberger, P. Gumbsch, *ACS Appl. Mater. Interfaces* ***8*****,** 15809 (2016).
97. D.A. Rigney, S. Karthikeyan, *Tribol. Lett.* **39**, 3 (2009).
98. H.M. Cao, X. Zhou, X.Y. Li, K. Lu, *Tribol. Int.* **115,** 3 (2017).
99. K. Wolff, Z. Liu, D. Braun, J. Schneider, C. Greiner, *Tribol. Int.* **102,** 540 (2016).
100. Z. Liu, C. Patzig, S. Selle, T. Höche, P. Gumbsch, C. Greiner, *Scr. Mater.* **153,** 114 (2018).
101. S.J. Eder, U. Cihak-Bayr, C. Gachot, M. Rodríguez Ripoll, *ACS Appl. Mater. Interfaces* **10,** 24288 (2018).
102. T. Sato, T. Ishida, L. Jalabert, H. Fujita, *Tribol. Online* **6**, 226 (2011).
103. B. Bhushan, *Fundamentals of Tribology and Bridging the Gap between the Macro-and Micro-/Nanoscales* (Springer Science and Business Media, Netherlands, 2012).